Effect of Ti insertion in the silicalite framework on the vibrational modes of the structure: An ab initio, and vibrational study

ARTICLE *in* STUDIES IN SURFACE SCIENCE AND CATALYSIS · DECEMBER 2001

DOI: 10.1016/S0167-2991(01)80149-X

7 AUTHORS, INCLUDING:

Gabriele Ricchiardi
Università degli Studi di Torino
89 PUBLICATIONS **4,307** CITATIONS

SEE PROFILE

Fulvio Ricci
Sapienza University of Rome
400 PUBLICATIONS **5,230** CITATIONS

SEE PROFILE

Studies in Surface Science and Catalysis 140
A. Gamba, C. Colella and S. Coluccia (Editors)

Effect of Ti insertion in the silicalite framework on the vibrational modes of the structure: an *ab initio*, and vibrational study

A. Damin[a], G. Ricchiardi[a], S. Bordiga[a], A. Zecchina[a], F. Ricci[b], G. Spanò[b] and C. Lamberti[a,c]

[a]Dipartimento di Chimica IFM, Via P. Giuria 7, I-10125 Torino, Italy
[b]EniChem S.p.A., Centro Ricerche Novara, "Istituto Guido Donegani", Via G. Fauser 4, 28100 Novara, Italy
[c]INFM Unità di Ricerca di Torino Università

We report a thorough theoretical study based on both "conventional" cluster and embedded cluster models on the effect induced on the vibrational modes of the MFI framework by the isomorphous insertion of a Ti atom. On an industrial ground, this insertion has generated one of the most important catalyst of the last two decades: titanium silicalite (TS-1). To allow a direct comparison of TS-1 with the parent Ti-free structure (silicalite), quantum chemical calculations on both cluster models $Ti[OSi(OH)_3]_4$ and $Si[OSi(OH)_3]_4$ have been performed. In both cases we have employed the B3LYP/6-31G(d) level of theory in order to provide the basis for the assignment of the main vibrational contributions. On an experimental ground, dehydrated TS-1 exhibits a IR spectrum characterized by a well defined band located at 960 cm^{-1} and a Raman spectrum showing two components at 960 and 1125 cm^{-1}, being the latter enhanced in case of resonant Raman effect achieved using an UV laser source. In this work, the enhancement of the intensity of the 1125 cm^{-1} feature and the invariance of the 960 cm^{-1} feature in UV-Raman experiments, are discussed in terms of resonant Raman selection rules. The resonance-enhanced 1125 cm^{-1} mode is unambiguously associated with a totally symmetric vibration of the TiO_4 tetrahedron, achieved through in-phase antisymmetric stretching of the four connected Ti-O-Si bridges. This vibration can also be described as an in-phase stretching of the four Si-O bonds pointing towards Ti. The resonance enhancement of this feature is explained in terms of the electronic structure of the Ti-containing moiety. Asymmetric stretching modes of TO_4 units show distinct behavior when T is occupied by Si or Ti, or when the oxygen atom belongs to OH groups (such as in terminal tetrahedra of cluster models and in real defective zeolites). Asymmetric SiO_4 and TiO_4 stretching modes appear above and below 1000 cm^{-1} respectively, when they are achieved through antisymmetric stretching of the T-O-Si bridges, and around 800 cm^{-1} (in both SiO_4 and TiO_4) when they involve symmetric stretching of the T-O-Si units. In purely siliceous models, the transparency gap between the main peaks at 800 and 1100 cm^{-1} contains only vibrational features associated with terminal Si-OH groups, while in Ti- containing models it contain also the above mentioned asymmetric TiO_4 modes, which in turn are strongly coupled with Si-OH stretching modes. Calculations on periodic models of silicalite and TS-1 free of OH groups using the QMPOT embedding method, correctly reproduce the transparency gap of silicalite and the appearance of asymmetric TiO_4 vibrations at 960 cm^{-1} in TS-1.

1. INTRODUCTION

Titanium silicalite-1 (TS-1) is a synthetic zeolite [1] in which a small number of Ti atoms substitute tetrahedral Si atoms in a purely siliceous framework with the MFI structure. It is an active and selective catalyst in a number of low-temperature oxidation reactions with aqueous H_2O_2 as the oxidant [2,3]. For this reason, it has been one of the most studied materials in heterogeneous catalysis in the last years. Although the long range structure of the material is well known [4,5] the structure of the active site is not clear. Several experimental [4-17] and computational [6-18-25] results demonstrate that the substitution of Si by Ti is isomorphous, and it is generally believed that the distribution of Ti over the available framework sites is at least partially disordered [5,15]. A variety of techniques has been developed, able to detect and discriminate tetra-coordinated framework titanium from extraframework titanium atoms with higher coordination. Among these we cite vibrational spectroscopies (both IR and Raman) [6-11], UV-Vis [11-13], EXAFS and XANES [11-15], spectroscopies and powder diffraction experiments (using both x-rays and neutrons) [4,5]. The first two methods in particular, due to their ease of use, have become standard analysis techniques for catalysts containing titanium. The infrared feature which is more clearly associated with the presence of tetrahedrally coordinated framework Ti is a relatively strong absorption appearing, in dehydrated samples, at 960 cm^{-1}. This work is focused on the vibrational peculiarities of the TS-1 material, as a consequence, a particular attention will be devoted to the history of the 960 cm^{-1} band.

The earlier interpretation of the 960 cm^{-1} band [7] was based on the discussion of the modes of isolated SiO_4 tetrahedra as compared with tetrahedra neighboring with a TiO_4 unit. Assuming a higher ionicity of the Ti-O bond as compared with the Si-O one (later confirmed by quantum mechanical calculations), the Si-O stretching mode was expected to shift downwards due to the interaction with the Ti cation ($Si\text{-}O^{\delta-}...Ti^{\delta+}$). Based on quantum mechanical calculations on cluster models, it was later proposed, by de Man and Sauer, [20], that the mode is a simple antisymmetric stretching of the Si-O-Ti bridge. Indeed the two assignments may be seen as coincident, because they describe the same physical mode by focusing on different "building units" [7,8,26]. Smirnov and van de Graaf [21] calculated the vibrational spectra of a periodic model of TS-1 with molecular dynamics techniques. Their results support the localized Ti-O-Si nature of the 960 cm^{-1} vibration, but they also put into evidence the inequivalence of the Si-O and Ti-O bonds and show that the Si-O stretching gives the greater contribution to the vibration. Taking this into consideration, the assignment of the band to a $Si\text{-}O^-$ vibration in defects, proposed by Camblor *et al.* [27] is not exclusive of the previous assignments. In this work we will also show that the vibrational features of framework Ti and of defect sites are strongly coupled.

Raman spectroscopy revealed that the 960 cm^{-1} band is not the only vibrational feature appearing upon insertion of Ti in the MFI framework. Scarano *et al.* and the group of Jacobs [8] have observed a Raman active mode at 1125 cm^{-1} not present in the Ti-free silicalite and attributed to the insertion of Ti in the framework. This band was not observed in the IR spectra because totally overshadowed by the intense antisymmetric stretching of the Si-O-Si unit. More recently, Li *et al.* [10] have reported that the intensity of the 1125 cm^{-1} Raman band is remarkably enhanced using an UV laser as scattering source. The reason of this effect is due to the strong Ligand to Metal Charge Transfer (LMCT)

absorption that TS-1 exhibits in the UV region of the electromagnetic spectrum, due to the $O^{2-}Ti^{4+} \rightarrow O^{-}Ti^{3+}$ transition. Li *et al.* have so operated in resonant Raman conditions. In such condition, no enhancement of the 960 cm^{-1} band was observed.

Resonant Raman spectroscopy is defined as a Raman experiment in which the exciting wavelengths coincides or is near to the wavelength of an electronic adsorption of the sample. This condition guarantees a high energy transfer to the sample, with minor disturbance by fluorescence. If the electronic absorption is due to a localized center, like a transition metal atom, excitation is also partially localized and the vibrational features of the immediate vicinity of the absorbing atom can be enhanced, if they meet the appropriate selection rules. This enhancement can be of several orders of magnitude. Besides the normal Raman selection rules, peculiar selection rules apply to the intensity enhancement. In particular, two kinds of vibrations are enhanced: a) totally symmetric vibrations with respect to the absorbing center, and b) vibrations along modes which cause the same molecular deformation caused by the electronic excitation [28].

In order to understand why the 1125 cm^{-1} band is enhanced in resonant Raman conditions, while the 960 cm^{-1} band is not, a careful comparison of the IR, Raman and resonant-Raman spectra of TS-1 samples at increasing Ti loading x (including a Ti-free silicalite sample, $x = 0$), coupled with quantum mechanical calculations on model compounds is needed. This study will give information on the symmetry of the modes involving the Ti atom.

2. METHODS: CLUSTERS AND EMBEDDED CLUSTER MODELS

Geometry optimization and vibrational frequency calculation of cluster models were performed both with the Hartree-Fock and density functional methods using the B3LYP functional. The basis set adopted is the standard 6-31G(d) in all cases. The program used was Gaussian98 [29] with Molden as the graphical interface [30] Because our HF frequencies are in good agreement with the B3LYP ones when scaled in the usual way (scale factor 0.9), in the following we will discuss only the unscaled B3LYP results. In models containing several dangling OH groups, the SiOH bending vibrations were strongly coupled with the Si-O and Ti-O stretching modes. In order to simplify the analysis of the latter, in some cases we substituted ^{1}H with ^{3}H in OH groups in order to decouple their bending vibrations. This led to small shifts of the Si-O and Ti-O vibrations (2-5 cm^{-1} was typical). For sake of completeness we report both the results obtained with terminal ^{1}H and ^{3}H atoms.

Embedded cluster calculations were performed with the QMPOT method [31], coupling a quantum mechanical description of a core set of atoms with a molecular mechanics description of the periodic solid. The QM cluster was treated at the Hartree-Fock level with a split valence SVP basis set [32]. The periodic solid was described with a shell model potential parametrized on QM calculations using the same level of theory. The choice of different methods and basis sets for the cluster and embedded cluster calculations was dictated by the availability of the forcefield for Ti-O interactions. The programs used for the calculation of the subsystems were Gaussian98 [29] and GULP [33], InsightII [34] was the graphical interface program. Periodic vibrational frequencies were calculated for k=0 (858 modes) and converted into an approximate density of states by assigning a gaussian shape with constant width (10 cm^{-1}) and area, and summing over all modes.

3 EXPERIMENTAL: SYNTHESIS AND SPECTROSCOPY

Samples with increasing Ti content have been synthesized in EniChem laboratories following a procedure described in the original patent [1]. The total insertion of Ti atoms in the MFI framework has been witnessed by comparison of the amount of Ti found in the samples by chemical analysis with the cell volumes obtained by Rietveld refinement of powder XRD data, see Ref. [4] for more details.

For IR spectra a Brucker IFS 66 FTIR spectrometer equipped with an HgCdTe cryodetector has been used. For all spectra a resolution of 2 cm^{-1} has been adopted. Samples have been studied in transmission mode on thin self-supported wafers. Adsorbates have been dosed in gas phase through a vacuum manifold directly connected with the measure cell.

The "conventional" Raman spectra were obtained on a Perkin Elmer 2000 NIR-FT Raman spectrometer equipped with an InGaAs detector. The lasing medium was an Nd-YAG crystal pumped by a high-pressure krypton lamp, resulting in an excitation wavelength of 1064 nm (9385 cm^{-1}). The power output was ca. 1000 mW. Samples were examined as such or contacted with solutions.

UV resonance Raman spectra were obtained using a Renishaw Raman System 1000 by exciting with a frequency doubled Ar^{+}-laser, operating at 244 nm (40984 cm^{-1}). The photons scattered by the sample where dispersed by the monochromator and simultaneously collected on an UV-enhanced CCD camera. The collection optic was a x40 objective. A laser output of 12 mW was used, which resulted in a maximum incident power at the sample of approximately 2 mW. An exposure time of 240 s per spectrum was used.

4. RESULT AND DISCUSSION

4.1. *Ab initio* study

Cluster models have been previously used to interpret the vibrational features of titanosilicates. In particular, Sauer and de Man [20] have calculated the vibrational spectra of a variety of small clusters, demonstrating that antisymmetric Ti-O-Si vibration may appear at frequencies around 960 cm^{-1}. However, the occurrence and exact frequency of these vibrations vary widely with model size and connectivity, in a manner which has not yet been explained. The interpretation of the vibrational structure of cluster models containing open chains is much complicated by the strong coupling of the T-O stretching modes with the bending modes of terminal hydroxyls. This problem can be overcome by adopting clusters formed by closed rings: however, if small or condensed rings are adopted (*e.g.* four-membered), the strain imposed by ring closure completely alter the vibrational features in the region of interest (700-1200 cm^{-1}). In this work, we focus on one type of cluster - a central tetrahedron surrounded by four complete tetrahedra, also known as "shell-3" model because it contains three complete shells of neighbors of the central atom - and refine the discussion of ref. [20] in three directions. First, we have improved the accuracy of the calculations for the isolated cluster, by using Density Functional theory and the 6-31G(d) basis set. Secondly, we have simplified the interpretation of the results by using isotopic substitution (^{1}H substituted with ^{3}H) to eliminate the coupling of Si-O-H

bending modes with Si-O and Ti-O stretching modes. Finally, we have attempted the calculation of the vibrational spectrum of a true periodic model of TS-1, by embedding the above-mentioned cluster into a periodic lattice treated with empirical potentials.

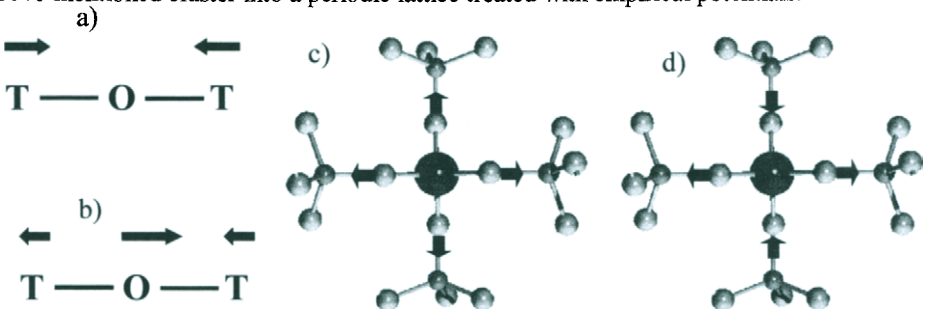

Scheme I. Representation of the symmetric and antisymmetric stretching modes of the T-O-T unit, parts (a) and (b) respectively. Symmetric and antisymmetric stretching modes of the TO_4 unit, parts (c) and (d) respectively.

$Si(OSi(OH)_3)_4$ and $Ti(OSi(OH)_3)_4$ clusters (named *SiSi4* and *TiSi4* in the following) have been used. The calculated frequencies in the 800-1200 cm^{-1} are reported in Table 1 and 2 respectively. The calculated modes can be analyzed according to the symmetry of the vibration around the central atom of each tetrahedron or according to the symmetry of the T-O-T bridge deformation, *i.e.* whether the two bonds stretch in phase or not (Scheme Ia,b). In the case of this second classification, we can further separate the modes according to the symmetry of the deformation of the four T-O-T bridges around the central cluster atom. An example is given in Scheme I. In Scheme Ic) the totally symmetric stretching mode of the internal tetrahedron is represented, which can be also seen as an in-phase combination of four T-O-Si antisymmetric modes, or if we neglect the central atom or consider it like a simple perturbation like an in-phase stretching of the four neighbouring Si-O oscillators. In Scheme Id) one of the asymmetric modes of the central tetrahedron is represented, which can be also described as an out-of-phase combination of four T-O-Si bridges or neighboring Si-O bonds. We will see later that these modes have different responses to the Si/Ti substitution. The main spectroscopic features of the *SiSi4* and *TiSi4* models are described in Tables 1 and 2 together with their assignment in terms of vibrations of TO_4 or T-O-Si units.

In the computed spectra of both of *SiSi4* and *TiSi4*, clusters, the highest modes are represented by stretching modes of the central atom of the cluster. In the case of *TiSi4*, only one stretching of the central tetrahedron falls in this region, which is also an in-phase antisymmetric stretching of the four TiOSi bridges (1097 cm^{-1}). Due to his symmetry around the Ti atom, this mode is the only candidate for the assignment of the 1125 cm^{-1} Raman band observed experimentally, see Introduction and *vide infra*. The mode also appear at similar frequencies in closed ring clusters (not reported) and can be regarded as the main Raman fingerprint of tetrahedral titanium. It is completely IR-inactive due to its symmetry. The analogous mode for *SiSi4* is observed at 1159 cm^{-1}. When the symmetric deformations of TO_4 involve symmetric T-O-Si stretching, modes at 827 and 814 cm^{-1} are computed for *SiSi4* and *TiSi4* respectively.

Table 1. Computed stretching frequencies for the $Si[OSi(OH)_3]_4$ model (ν), and symmetry of the corresponding mode with respect to the central SiO_4 and Si-O-Si unit. A = antisymmetric and S = symmetric.

$\nu(cm^{-1})$	SiO_4	Si-O-Si	Comments
1159	S	A	See text
1105,1096	A	A	See text
996, 984, 971	-	-	Si-O stretching modes of terminal silanols involved in hydrogen bonds with neighboring OH as donors.
993	-	-	Si-O stretching modes of terminal silanol (no H-bond)
917	-	-	Si-O stretching modes of terminal silanol in which O is hydrogen bond acceptor.
876, 855	A	S	See text
827	S	S	See text

Table 2. Computed stretching frequencies for the $Ti[OSi(OH)_3]_4$ model (ν), and symmetry of the corresponding mode with respect to the central TiO_4 and T-O-T unit. A = antisymmetric and S = symmetric.

$\nu(cm^{-1})$	TiO_4	Ti-O-Si	Comments
1097	S	A	See text
987, 964	-	-	Si-O stretching modes of terminal silanols involved in hydrogen bonds with neighboring OH as donors.
986, 968, 965,909, 897	A	A	Ti-O stretching modes strongly coupled with Si-O stretching modes of terminal silanols involved in H-bonds with neighboring OH as donors.
913	-	-	Si-O stretching modes of terminal silanols involved in hydrogen bonds with neighboring OH as acceptors
829, 824	A	S	See text
814	S	S	See text

If we consider now the asymmetric deformations of the central tetrahedron (occupied by Ti or Si), the two models are much different. The asymmetric deformations of SiO_4 in *SiSi4* produce features at 1105 and 1096 cm^{-1} when they occur through antisymmetric Si-O-Si stretching. On the contrary, TiO_4 asymmetric vibrations in *TiSi4*, appear below 1000 cm^{-1} (multiplet at 986, 968, 965, 909 and 897 cm^{-1}). When the asymmetric deformations of TO_4 involve symmetric T-O-Si stretching, modes at 876, 855 cm^{-1} and at 829, 824 cm^{-1} occur for *SiSi4* and *TiSi4* respectively. This fact lead us to the discussion of the bands appearing in the central region of the spectra (850-1000 cm^{-1}), *i.e.* in the experimentally observed "gap" between the high-frequency (1250-1050 cm^{-1}) antisymmetric Si-O-Si vibrations and the low frequency (around 800 cm^{-1}) symmetric Si-O-Si vibrations, see Figs. 1,2. This region is of much interest, because it contains: i) the

highly debated 960 cm^{-1} band observed in both IR and Raman spectra; ii) the features associated with framework defects.

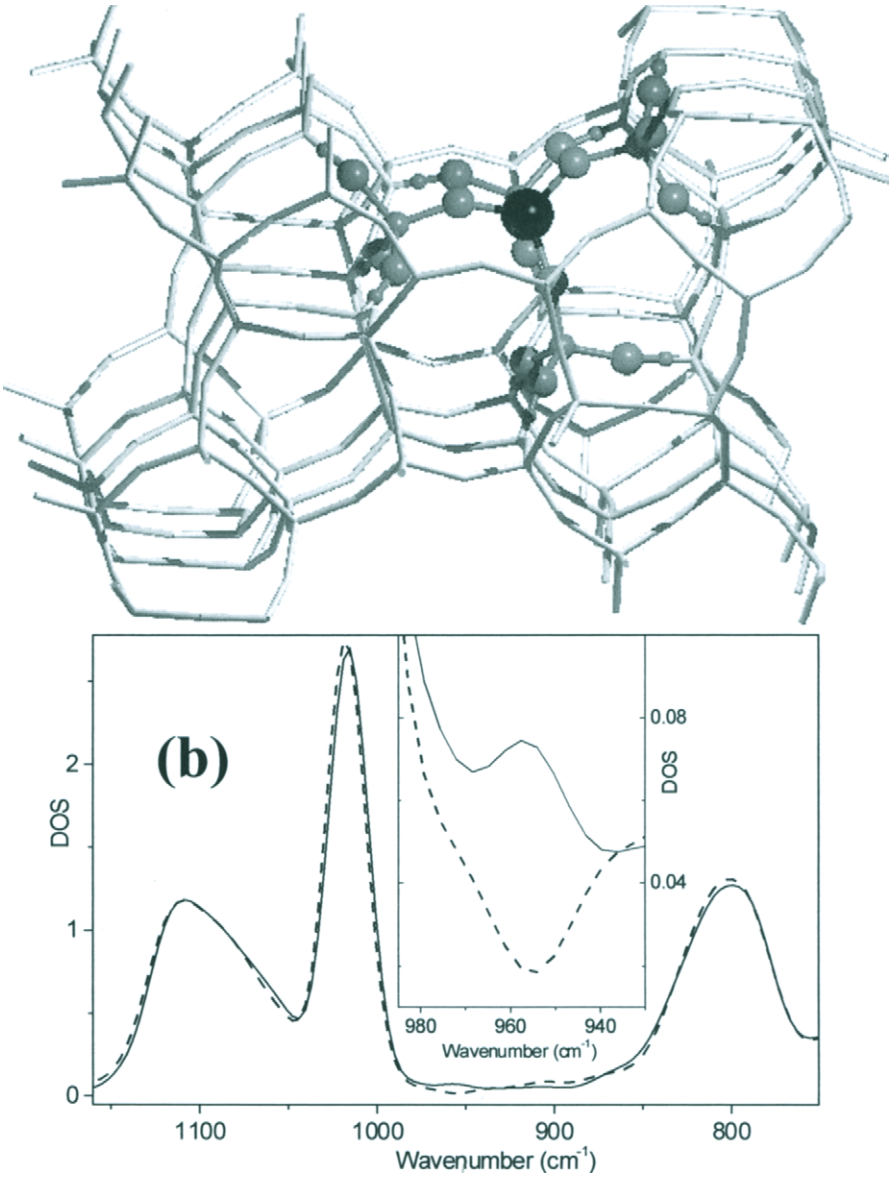

Fig. 1. Part (a): graphical representation of the periodic model used in this study. The shell-3 clusters has been embedded into the crystallographic T5 position. Part (b): the so obtained DOS for the silicalite (dashed line) and for TS-1 (full line). The inset reports a magnification of the of the two curves in the gap between the symmetric and antisymmetric stretching modes of the T-O-T units, highlighting the appearance of the 960 cm^{-1} band for TS-1, otherwise hardly visible.

The calculated spectrum of *SiSi4* in this region contains only Si-O stretching modes associated with terminal Si-OH groups of the models. These modes are spread over a wide range (917-996 cm^{-1}) because of the different hydrogen bonds involving the terminal OH groups of the cluster. These modes are good candidates to interpret the IR modes appearing in the gap of defective silicates (*e.g.* defective silicalite) [27,35,36]. No stretching modes of the central tetrahedron appear in this region. This is confirmed by our calculation on the periodic model (*SiSi4* embedded in the periodic structure), which correctly reproduce the experimentally observed gap between 850 and 1000 cm^{-1} (Fig. 1b *vs.* dashed line in Fig.2).

In the case of *TiSi4* cluster, the Si-OH stretching modes are strongly coupled with asymmetric TiO_4 stretching modes. These modes are out-of-phase combinations of the four Ti-O-Si antisymmetric stretching. They also span a wide frequency range (897-986 cm^{-1}), and no single mode can be associated individually to the 960 cm^{-1} band. This clearly show on one hand, that our cluster is inadequate to model a non-defective titanosilicate, and on the other hand, that in defective titanosilicates the Si-OH and asymmetric TiO_4 vibrations are strongly coupled. This is why spectroscopic features in this range are still under debate [10].

The modeling a non-defective titanosilicate thus requires either larger clusters or a periodic model. We have embedded the shell-3 clusters into the crystallographic T5 position of a unit cell of the MFI framework (Fig. 1a). In the case of the embedding of the *SiSi4* cluster, the resulting structure is purely siliceous, while for the *TiSi4* cluster, we obtain a structure with one Ti atom per unit cell. No hydroxy groups are present in either model. The choice of the T5 position is partly arbitrary, and dictated by the availability of the calculated structure from a previous work [25]. Fig. 1b reports the calculated density of states of Silicalite and TS-1. The DOS of silicalite correctly reproduce the two main groups of framework vibrations centered at 800 and 1100 cm^{-1}, and the transparency region between them. The DOS of Ti-silicalite is very similar but differs for a small, expected [1,6-9,11], feature at 960 cm^{-1}. Graphical analysis of the individual normal modes contributing to the DOS at this frequency shows four contributions: two modes involving antisymmetric stretching of Si-O-Si bridges far from the Ti atom and two modes which can be classified as out-of-phase asymmetric stretching of the Ti-O-Si bridges. The former have no counterpart in cluster calculations and may be artifacts due to a faulty modeling of the interface between the QM and MM regions, while the latter are in full agreement with the cluster calculations and with the assignment of the 960 cm^{-1} band presented above. This result, although not conclusive due to the limitations of the model, indicates that the embedding of the *TiSi4* cluster into a non-defective periodic framework causes the disappearance of the scattered (897-987 cm^{-1}) bands due to coupled Ti-O-Si-OH vibrations and the appearance of a single narrow band at 960 cm^{-1}.

Quantum mechanical calculations not only provides vibrational frequencies to be compared with the experimental ones, but also describe the electronic structure of the clusters, which has deep implications in the Resonant Raman experiments. In particular, the structure and symmetry of the LUMO of the Ti-containing clusters have to be considered (an accurate calculation of the true electronic structure of the excited state is beyond the scope of the present work). The LUMO of the *TiSi4* cluster is almost totally symmetric around the Ti atom and two-fold degenerate. The LUMO is formed by an antibonding combination of O *p* orbitals with a totally symmetric combination of Ti *d* orbitals ($d(z^2)$, $d(x^2-y^2)$).

It is reasonable to deduce that the observed UV absorption at 205 nm (about 49000 cm^{-1}) involves a totally symmetric excited state in which all four Ti-O bonds are symmetrically stretched with respect to the ground state (due to the Ti-O antibonding character of the LUMO). Thus the symmetric TiO_4 stretching meets both selection rules a) and b) (see the introduction) for the resonance enhancement of its Raman intensity. We therefore conclude that the observed band at 1125 cm^{-1} (calculated at 1100 cm^{-1} in the *TiSi4* cluster) can be attributed to this kind of vibration. Based on the discussion above, this vibration can be also described as the in-phase combination of the four Ti-O-Si stretching modes, or as the in-phase combination of the four $Si\text{-}O^{\delta-}$ bonds perturbed by Ti.

On the contrary, none of the vibrations appearing in the "gap" meets either of the selection rules for Raman enhancement. This explain why the 960 cm^{-1} band is not enhanced. Indeed, it apparently disappears in Resonant experiments due to the enormous intensity of the strongly enhanced 1125 cm^{-1} band. Nevertheless, the Ti-sensitive nature of the 960 cm^{-1} band is confirmed by non-resonant experiments, as discussed in the previous sections.

4.2. Evidence of the correlation of the 1125 and 960 cm^{-1} bands with Ti content

In this experimental section we will prove that both the IR active 960 cm^{-1} band and the Raman active 1125 cm^{-1} bands have an intensity which is linearly correlated with the Ti content of TS-1 samples. The use of resonant Raman will testify that the latter band is enhanced according to the assignments discussed in our quantum chemical study.

Fig. 2 reports, in a wide spectroscopic range (3800-700 cm^{-1}), the IR feature of both silicalite (dashed spectrum) and TS-1 (solid spectrum). The two spectra look almost identical, being the only significant difference the narrow 960 cm^{-1} band visible in the upper right corner of the figure and magnified in the inset (which also allow a direct comparison with the computed DOS reported in Fig. 1b). It becomes now evident that the 960 cm^{-1} band is a small, although significant, feature of the overall spectrum of TS-1. This band lies in the gap between the symmetric and asymmetric stretching modes of the T-O-T units, the latter totally saturated. At higher frequencies, the stretching of hydroxyls are visible: sharp peak at 3737 cm^{-1} and broad component around 3475 cm^{-1}, which are due to isolated and H-bonded Si-O-H (and probably to Ti-O-H) species respectively. In particular, the latter component implies that TS-1 is a defective material (as silicalite is), hosting an important fraction of T vacancies, generating internal hydroxylated cavities [35-37]. At 2005, 1180 and 1640 cm^{-1} the overtone and combination bands are also visible.

To validate the attribution of the vibrational modes done in section 4.1, Raman, resonant Raman and IR spectra on a set of TS-1 samples characterized by an increasing Ti loading (x) are reported in Figure 3. Part a) of the figure reports spectra collected on three samples (x = 3.0, 1.4 and 0.0 *i.e.* silicalite) with a FTIR Raman spectrometer [λ_{laser} = 1064 nm (9385 cm^{-1})], while part b) of the figure shows spectra obtained with a dispersive instrument working with a λ_{laser} = 244 nm (40984 cm^{-1}). With the latter experimental setup we are in resonant Raman conditions for the $O^{2-}Ti^{4+} \rightarrow O^{-}Ti^{3+}$ LMCT. In fact, for tetrahedral coordinated Ti^{4+} this LMCT exhibits an absorption band centered around 205 nm (about 49000 cm^{-1}) with a low energy tail extending down to 250 nm (40000 cm^{-1}) [11,12], see inset in Fig. 3b. The Raman spectrum of silicalite sample is very similar independently on the used laser source, showing bands at 1230, 1085, 975 cm^{-1} and a complex absorption centered at 820 cm^{-1}. In fact no resonant enhanced effect is expected

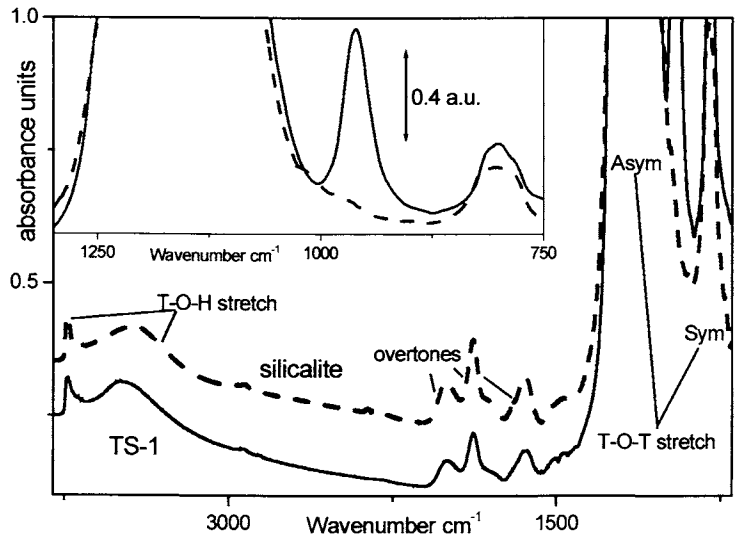

Fig. 2. Comparison between the IR spectra in the 3800-700 cm^{-1} range of silicalite (dashed line) and TS-1 (full line). The inset reports the magnification of the framework stretching region, to be compared to DOS reported in Fig. 1b.

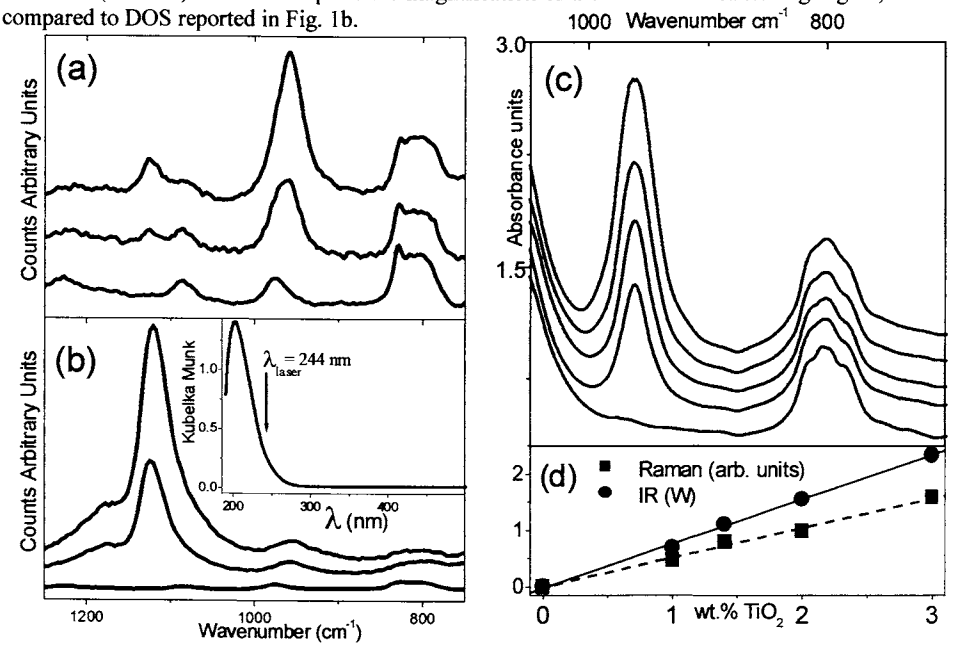

Fig. 3. Part (a): Raman spectra of TS-1, from top to bottom $x = 3.0$, 1.4 and 0.0 (silicalite). Part (b): as part for resonant Raman. The inset reports the DRS spectra of TS-1; the vertical arrow shows the wavelength of the UV laser source. Part (c): IR spectra of TS-1, from top to bottom $x = 3.0$, 2.0, 1.4, 1.0 and 0.0. Part (d) intensity of the 960 cm^{-1} band vs. x, in (non resonant) Raman (■) and IR (●) spectra. For the latter, the height W at FWHM of band is reported, see text.

for a sample transparent at the excitation wavelength, occurring the $O^{2-}Si^{4+} \rightarrow O^{-}Si^{3+}$ LMCT at much higher energies. The bands at 1230 and 1085 cm^{-1} have been associated to $\nu_{asym.}$(Si-O-Si) (Raman inactive) [8a] while the stronger absorption at 975 cm^{-1} has been assigned to $\nu_{asym.}$(Si-O-Si*) where Si* is a silicon atom connected with an hydroxy-group $Si[OSi]_3OH$ [8a]. The fact that this component, characteristic of defective silicalite, occurs close to the 960 cm^{-1} band of TS-1 is probably the origin of the animated debate on the nature of this band (see Introduction). Finally the complex absorption centered at 820 cm^{-1} has been associated with the $\nu_{sym.}$(T-O-T) (Raman active) [8a]. Moving now to TS-1 samples we observe, two main differences: i) the appearance of a new band at 1125 cm^{-1} which is enhanced by resonant Raman effect (compare Fig. 3b *vs.* 3a); ii) the growth of a band at 960 cm^{-1} which intensity is proportional to *x*, see Fig. 3d. For both resonant (Fig. 3b) and non-resonant Raman (Fig. 3a), the constant value of I(1125)/I(960) ratio (0.25 and 11 respectively, independently to *x*) indicates that the two bands should be related to two different spectroscopic manifestations of the same phenomenon: insertion of Ti in the MFI framework.

Even if the 960 cm^{-1} band is generally recognized as a proof that Ti(IV) heteroatoms are isomorphically inserted in the zeolite structure [6-8,11], a quantitative correlation between the Ti content (*x*) and the intensity of the 960 cm^{-1} IR band is very critical. On an experimental ground this is due to its great intensity at high Ti content and to the fact that it is modified, in both intensity and position, by adsorbed molecules. For this reasons, great care has been made in order to prepare TS-1 pellets as thin as possible and to measure TS-1 samples that have undergone the same dehydration treatment. Fig. 3c reports the IR spectra of five TS-1 samples containing increasing Ti content *x*, from x = 3.0 down to x = 0.0, pure silicalite (bottom curve). The spectra have been normalized on the overtone crystal modes, *i.e.* considering the bands in the 2000-1500 cm^{-1} range (see Fig. 2). The quality of the normalization procedure is confirmed by the good superposition of the spectra in the 750-850 cm^{-1} range, which is also not influenced by Ti content. The common method of dilution with KBr can not be used for reducing the absorbance intensities of the framework modes, since it does not allow thermal treatments, which are needed in order to remove the adsorbed water. In fact, the 960 cm^{-1} band is affected in its shape, frequency and intensity according to the amount of weakly adsorbed basic molecules.

We assume that: (i) the 960 cm^{-1} band does not saturate for the TS-1 sample with lowest Ti content; and (ii) the "true" Full Width at Half Maximum (FWHM) of this band is constant over all set of TS-1 samples. The former assumption is supported by the fact that the intensity of the 960 cm^{-1} band, for the $x = 1.0$ sample, is less than 1.5 in absorbance units, while the latter is exactly what expected for a band associated to different concentrations of a unique species. Assumption (i) allows us to measure the "true" FWHM of the 960 cm^{-1} band in TS-1 samples (27 cm^{-1}). Now, following assumption (ii), we were able to estimate for all samples reported in Fig. 3, the absorbance (W) at the height where the width of the band corresponds to 27 cm^{-1}. This method minimize the errors due to the instrument sensibility and allows a quantitative estimation of the band intensity. Such obtained values plotted against *x* in the Fig. 3d (• data), give a high linear correlation (r = 0.9998) and validate assumption (i) and (ii). A further, and definitive, validation comes from the similar linearity found for the intensities of the Raman band, which can not be affected by saturation problems, see Fig. 3d (▪ data). These results implies that the 960 cm^{-1} band is well a fingerprint of the insertion of Ti in the zeolitic framework, even if not

enhanced by Raman resonant spectroscopy for the reasons outlined in our theoretical study (section 4.1). Thus the original interpreatation of our group [6-8,11] is confirmed and the assignment of the 960 cm^{-1} band to the presence of defects [10] is rejected.

5. CONCLUSIONS

This work discusses the vibrational features associated with the insertion of tetrahedral Ti in the MFI zeolite lattice. The understanding of these features forms the base for the technical characterization of Ti containing silicate catalysts using spectroscopic methods, which is of capital importance in industrial catalysis. A combination of spectroscopic and computational techniques is used in order to assign the main vibrational features of Ti-silicalite, also taking into account the presence of hydroxylated defects.

A set of experiments on TS-1 samples with variable Ti content, synthesized and treated in a reproducible way, has allowed to proof the quantitative correlation between Ti content and the intensity of the 960cm^{-1} IR feature. The linear correlation between the intensity of the 960cm^{-1} band and x has been also confirmed by Raman spectroscopy.

Raman experiments on silicalite and TS-1 with excitation wavelengths of 1064 nm (non resonant) and 244 nm (resonant) show that: (i) the main features associated with Ti insertion in the lattice are vibrations at 1125 and 960 cm^{-1}; the former being drastically enhanced by UV-resonance, while the latter is not; (ii) a mode is observed at 978 cm^{-1} on defective silicalites and TS-1, which we attribute to the Si-O stretching in silanols. The proximity of the 960 and 978 cm^{-1} modes has prompted us to re-examine IR spectroscopy in the same region in order to distinguish the 960 cm^{-1} band from defect modes.

Quantum mechanical calculations of the vibrational frequencies and electronic structure of shell-3 cluster models allow to assign the main vibrational features. The 1125 cm^{-1} peak is undoubtedly assigned to the symmetric stretching vibration of the TiO_4 tetrahedron, achieved through in-phase antisymmetric stretching of the four connected Ti-O-Si oscillators. According to its symmetry and to the electronic structure of the Ti moiety, this is the only vibration fulfilling the resonant Raman selection rules. This assignment is equivalent to the assignment to the in-phase stretching of the four Si-O bonds surrounding Ti. The asymmetric vibrations of TO_4 of our cluster models appear above 1000 cm^{-1} for SiO_4 and between 897 and 986 cm^{-1} for TiO_4. These modes are strongly coupled with the Si-O stretching of the silanols in the outer part of the cluster. Embedding of the Ti-containing cluster in a periodic silicalite framework makes the mode coalesce into a band centered at 960 cm^{-1}. In the purely siliceous model, the only modes contributing to this region are the Si-O vibrations of the silanols in the outer sphere. Based on these results, we confirm the assignment of the 960 cm^{-1} band to the asymmetric stretching of the TiO_4 unit, which can equivalently be described as the out-of-phase antisymmetric stretching of the four connected Ti-O-Si oscillators, or as the out-of-phase stretching of the four Si-O bonds pointing towards Ti.

REFERENCES

[1] M. Taramasso, G. Perego and B. Notari, US Patent No. 4410501 (1983).
[2] B. Notari, Adv. Catal. 41 (1996) 253, and references therein.

[3] G. Bellussi, A. Carati, G.M. Clerici, G. Maddinelli and R. Millini, J. Catal., 133 (1992) 220. M.A. Mantegazza, G. Leofanti, G. Petrini, M. Padovan, A. Zecchina and S. Bordiga, Stud. Surf. Sci. Catal. 82 (1994) 541; M.A. Mantegazza, G. Petrini, G. Spanò, R. Bagatin and F. Rivetti, J. Mol. Catal. A 146 (1999) 223.
[4] R. Millini, E. Previdi Massara, G. Perego and G. Bellussi, J. Catal., 137 (1992) 497; C. Lamberti, S. Bordiga, A. Zecchina, A. Carati, A.N. Fitch, G. Artioli, G. Petrini, M. Salvalaggio, G.L. Marra, J. Catal., 183 (1999) 222
[5] G. L. Marra, G. Artioli, A. N. Fitch, M. Milanesio and C. Lamberti, Microporous Mesoporous Mater., 40 (2000) 85; C.Lamberti, S.Bordiga, A.Zecchina, G. Artioli, G.L. Marra and G. Spanò, J. Am. Chem. Soc., 123 (2001) in press, and references therein.
[6] G. Tozzola, M.A. Mantegazza, G. Ranghino, G. Petrini, S. Bordiga, G. Ricchiardi, C. Lamberti, R. Zulian and A. Zecchina, J. Catal., 179 (1998) 64.
[7] M.R. Boccuti, K.M. Rao, A.Zecchina, G. Leofanti and G. Petrini, Stud. Surf. Sci. Catal., 48 (1989) 133.
[8] a) D. Scarano, A. Zecchina, S. Bordiga, F. Geobaldo, G. Spoto, G. Petrini, G. Leofanti, M. Padovan and G. Tozzola, J. Chem. Soc. Faraday Trans., 89 (1993) 4123; b) G. Deo, A. Turek, I.E. Wachs, D.R.C. Huybrechts and P. A. Jacobs Zeolites 13 (1993) 365.
[9] D.R. Huybrechts, P.L. Buskens and P.A. Jacobs, J. Mol. Catal. 71 (1992) 129; A.J. van der Pol, and H.P. van Hooff, Appl. Catal. A, 92 (1992) 93.
[10] C. Li, G. Xiong, Q. Xin, J. Liu, P. Ying, Z. Feng, J. Li, W. Yang, Y. Wang, G. Wang, X. Liu, M. Lin, X. Wang, and E. Min, Angew. Chem. Int. Ed., 38, (1999) 2220.
[11] S. Bordiga, S. Coluccia, C. Lamberti, L. Marchese, A. Zecchina, F. Boscherini, F. Buffa, F. Genoni, G. Leofanti, G. Petrini, and G. Vlaic J. Phys. Chem., 98 (1994) 4125; S. Bordiga, F. Boscherini, S.Coluccia, F.Genoni, C. Lamberti, G. Leofanti, L. Marchese, G. Petrini, G. Vlaic and A. Zecchina, Catal. Lett. 26 (1994)195.
[12] C. Lamberti, S. Bordiga, D. Arduino, A. Zecchina, F. Geobaldo, G. Spanò, F. Genoni, G. Petrini, A. Carati, F. Villain and G. Vlaic, J. Phys. Chem. B, 102 (1998) 6382.
[13] D. Trong On, L. Le Noc and L. Bonneviot, Chem. Comm., (1996) 299.
[14] D. Gleeson, G. Sankar, C.R.A. Catlow, J.M. Thomas, G. Spanó, S. Bordiga, A. Zecchina, C. Lamberti, Phys. Chem. Chem. Phys., 2 (2000) 4812.
[15] V. Bolis, S. Bordiga, C. Lamberti, A. Zecchina, A. Carati, F. Rivetti G. Spanò and G. Petrini, Langmuir, 15 (1999) 5753; V. Bolis, S. Bordiga, C. Lamberti, A. Zecchina, A. Carati, G. Petrini, F. Rivetti and G. Spanò, Microporous Mesoporous Mater., 30 (1999) 67.
[16] R. Millini and G. Perego, Gazzetta Chimica Ital., 126 (1996) 133, and references therein.
[17] G.N. Vayssilov, Catal. Rev. Sci. Engl., 39 (1997) 209, and references therein.
[18] A. Jentys and C.R.A. Catlow, Catal. Lett., 22 (1993) 251.
[19] R. Millini, G. Perego and K. Seiti, Stud. Surf. Sci. Catal., 84 (1994) 2123.
[20] A.J.M. de Mann, and J. Sauer, J. Phys. Chem., 100 (1996) 5025.
[21] K.S. Smirnov and B. van de Graaf, Microporous Mater., 7 (1996) 133.
[22] P.E. Sinclair, G. Sankar, C.R.A. Catlow, J.M. Thomas and T. Maschmeyer, J. Phys. Chem. B, 101 (1997) 4237.
[23] C.M. Zicovich-Wilson, R. Dovesi and A.Corma, J. Phys. Chem. B, 103 (1999) 988.
[24] P.E. Sinclair and C.R.A. Catlow, J. Phys. Chem. B, 103 (1999) 1084.
[25] G. Ricchiardi, A.J.M. de Man and J. Sauer, Phys. Chem. Chem. Phys., 2 (2000) 2195.
[26] A.Miecznikowski and J. Hamuza, Zeolites, 7 (1987) 249; A.J.M. de Man, B.W.H. van

Beest, M. Leslie and R.A. van Santen, J. Phys. Chem., 94 (1990) 2524.
[27] M.A. Camblor, A. Corma and J. Perez-Pariente, J. Chem. Soc. Chem. Commun., (1993) 557.
[28] Y. Nishimura, A.Y. Hirakawa and M. Tsuboi, in R.J.H. Clark and R.E. Hester, (Eds.) Advances in Infrared and Raman Spectroscopy, Heyden & Son, London, 1978; P.R. Carey, Biochemical Applications of Raman and Resonance Raman Spectroscopies, Academic Press, New York, 1982 (and references therein).
[29] M.J. Frisch, G.W. Trucks, H.B. Schlegel, G.E. Scuseria, M.A. Robb, J.R. Cheeseman, V.G. Zakrzewski, J.A. Montgomery Jr., R.E. Stratmann, J.C. Burant, S. Dapprich, J.M. Millam, A.D. Daniels, K.N. Kudin, M.C. Strain, O. Farkas, J. Tomasi, V. Barone, M. Cossi, R. Cammi, B. Mennucci, C. Pomelli, C. Adamo, S. Clifford, J. Ochterski, G.A. Petersson, P.Y. Ayala, Q. Cui, K. Morokuma, D.K. Malick, A.D. Rabuck, K. Raghavachari, J.B. Foresman, J. Cioslowski, J.V. Ortiz, A.G. Baboul, B.B. Stefanov, G. Liu, A. Liashenko, P. Piskorz, I. Komaromi, R. Gomperts, R.L. Martin, D.J. Fox, T. Keith, M.A. Al-Laham, C.Y. Peng, A. Nanayakkara, C. Gonzalez, M. Challacombe, P.M.W. Gill, B. Johnson, W. Chen, M.W. Wong, J.L. Andres, C. Gonzalez, M. Head-Gordon, E.S. Replogle and J.A. Pople, Gaussian 98, Revision A.7, Gaussian, Inc., Pittsburgh PA, 1998.
[30] G.A. Petersson, A. Bennett, T.G. Tensfeldt, M.A. Al-Laham, W.A. Shirley and J. Mantzaris, J. Chem.Phys, 89 (1996) 2193.
[31] U. Eichler, C. Kölmel and J. Sauer, J. Comput. Chem., 18 (1997) 463; U. Eichler, M. Brändle and J. Sauer, J. Phys. Chem. B, 101 (1997) 10035.
[32] A. Schäfer, H. Horn and R. Ahlrichs, J. Chem. Phys., 97 (1992) 2571.
[33] J. Gale, J. Chem. Soc. Faraday Trans., 93 (1997) 629.
[34] InsightII 4.0.0 molecular modelling system. Molecular Simulation Inc., San Diego.
[35] A. Zecchina, S. Bordiga, G. Spoto, L. Marchese, G. Petrini, G. Leofanti and M. Padovan, J. Phys. Chem., 96 (1992) 4985; A. Zecchina, S. Bordiga, G. Spoto, L. Marchese, G. Petrini, G. Leofanti and M. Padovan, M. J. Phys. Chem., 96 (1992) 4991; A. Zecchina, S. Bordiga, G. Spoto, L. Marchese, G. Petrini, G. Leofanti, M. Padovan, C. Otero Areàn, J. Chem. Soc. Faraday Trans., 88 (1992) 2959; G.L. Marra, G. Tozzola, G. Leofanti, M. Padovan, G. Petrini, F. Genoni, B. Venturelli, A. Zecchina, S. Bordiga, G. Ricchiardi, Stud. Surf. Sci. Catal., 84 (1994) 559.
[36] S. Bordiga, P. Ugliengo, A. Damin, C. Lamberti, G. Spoto, A. Zecchina, G. Spanò, R. Buzzoni, L. Dalloro, F. Rivetti, Topics in Catal., (2001), in press; S. Bordiga, I. Roggero, P. Ugliengo, A. Zecchina, V. Bolis, G. Artioli, R. Buzzoni, G. L. Marra, F. Rivetti, G. Spanò and C. Lamberti, J. Chem. Soc. Dalton Trans., (2000) 3921.
[37] G. Artioli, C. Lamberti and G. L. Marra, Acta Cryst. B, 56 (2000) 2.